Relative Performance of Automatic Rain Gauges under Different Rainfall Conditions

JEFFREY A. NYSTUEN

Applied Physics Laboratory, University of Washington, Seattle, Washington

(Manuscript received 16 March 1998, in final form 9 October 1998)

ABSTRACT

Six different types of automatic rain gauges, including tipping bucket, weighing, capacitance, optical, disdrometer, and acoustical sensors, were deployed for 17 months (September 1993–January 1995) at the NOAA Atlantic Oceanographic and Meteorological Laboratory in Miami, Florida. Different rainfall conditions encountered during the experiment included wintertime stratiform frontal rainfall, intense springtime convective systems with extremely high rainfall rates (over 100 mm h^{-1}), summertime convective storms, mesoscale convective systems in the rainy season (September–October), and one tropical storm (Tropical Storm Gordon). Overall, all of the rain gauges performed well, with intercorrelations of order 0.9 or better using 1-min rainfall rates and biases of less than 10%; however, each showed limitations under different rainfall situations. In particular, under extremely heavy rainfall rates (over 100 mm h^{-1}), the disdrometer and tipping bucket rain gauges biased low, while the optical rain gauge biased high. Under light rainfall rates (under 2 mm h^{-1}), the capacitance and tipping bucket rain gauges showed significant instrument noise using the 1-min sampling interval. The optical gauge was sensitive to the relative proportion of small to large raindrops within the rain. The raindrop distribution parameter N_0, the coefficient of the exponential fit to the drop size distribution, could be used to predict the optical gauge bias. When N_0 is large (relatively more small drops), the optical gauge biases high, and when N_0 is small (relatively more large drops), the optical gauge biases low. The acoustic rain measurement showed significant variability when compared to the other gauges. The acoustic measurement is very sensitive to the presence of very large raindrops (over 3.5 mm diameter) as these raindrops are extraordinarily loud underwater and prevent the smaller drop size populations from being heard and accurately counted when they are present. While the range of wind speeds encountered during the experiment was limited, wind did affect the performance of several of the gauges. At higher wind speeds (over 5 m s^{-1}), the disdrometer and acoustic rain gauges biased low and the instrument noise of the capacitance gauge increased significantly.

1. Introduction

Because the distribution, type, and intensity of rainfall is now recognized to be a crucial component of many oceanographic, meteorological, and climate studies, extensive research efforts exist to identify new measurement techniques, including a recently launched dedicated satellite, the Tropical Rain Measuring Mission (TRMM). Potential methods for rainfall measurement include satellite techniques, weather radars, and various in situ rain gauges. Nevertheless, good quality rainfall measurements remain elusive because of the inherent spatial and temporal inhomogeneity of rainfall, and the difficulty of operating automatic instruments in remote regions and, especially, the oceanic environment.

Attempts to provide global estimates of the distribution of rainfall have been made using qualitative ship weather reports (e.g., Tucker 1961; Dorman and Bourke 1979; Reed and Elliot 1979; Legates and Willmott 1990; Petty 1995) and using satellite data (e.g., Arkin and Xie 1994; Barrett et al. 1994). Significant discrepancies between these efforts exist and extensive research into this topic is ongoing (Ebert et al. 1996). One of the biggest problems is the lack of adequate surface measurements of rainfall (Barrett et al. 1995). Generally, deployment of rain gauges on ships has not proven successful because of platform motion and ship-induced wind and exposure problems. Weather radars in coastal regions exist, however surface validation issues persist with these instruments and measurements are restricted to the few coastal areas where these expensive radars have been deployed.

Several types of automatic in situ rain gauges have been developed that show promise for deployment in remote regions, including at sea. These gauges include capacitance, optical, disdrometers, and acoustic systems. A few optical rain gauges have been deployed on deep ocean buoys (McPhaden and Milburn 1992) and the capacitance sensor is now part of the new instrument package for the National Oceanic and Atmospheric Administration (NOAA) Tropical–Atmosphere–Ocean

Corresponding author address: Dr. Jeffrey A. Nystuen, Applied Physics Laboratory, University of Washington, 1013 NE 40th Street, Seattle, WA 98105-6698.
E-mail: nystuen@apl.washington.edu

(TAO) array in the tropical Pacific Ocean (Milburn et al. 1996). Rainfall detection and measurement using hydrophones (underwater sound) deployed from drifting buoys has been demonstrated (Nystuen and Selsor 1997). These systems, plus two ''more traditional'' collection-type gauges (weighing and tipping bucket), were deployed at the Atlantic Oceanographic and Meteorological Laboratory (AOML) Rain Gauge Facility at Virginia Key, Florida. The experiment lasted from September 1993 through January 1995 (17 months), during which time roughly 800 rainfall events were recorded. A preliminary assessment of the rain gauge performances is found in Nystuen et al. (1996). Data collected from different types of rainfall events throughout the experimental period are examined to attempt to determine how different environmental conditions affect the performance of the different systems, including their potential for deployment at sea.

2. Describing rainfall

At the simplest level, rain is liquid water drops falling to the surface. Raindrops range in size from 200 μm to over 5 mm in diameter (Pruppacher and Klett 1978). The distribution of raindrop sizes varies considerably from rain to rain and has important implications. Different rainfall quantities, for example, rainfall rate, optical extinction, liquid water content, kinetic energy, and radar reflectivity (microwave backscatter), are all integral moments of the drop size distribution (Ulbrich 1983). The xth moment of the drop size distribution, M_x, is given by

$$M_x = \int D^x N(D)\, dD, \tag{1}$$

where $N(D)$ is the drop size distribution and D is the drop size. As different measurement instruments (collection type rain gauges, optical extinction, or scintillation gauges, radars, etc.) measure different moments of the drop size distribution, understanding the relationship between the measured quantity and the desired quantity is important (Atlas and Ulbrich 1974; Ulbrich and Atlas 1978). In this experiment, direct measurements of the drop size distribution by the disdrometer allows the performance characteristics of the different rain gauges to be examined under different rainfall conditions, as defined by drop size distribution.

The drop size distribution is often parameterized. The most common parameterization is an exponential distribution first described by Marshall and Palmer (1948):

$$N(D) = N_0 e^{-\Lambda D} \tag{2}$$

where N_0 varies and Λ is a function of rainfall rate. This form of drop size distribution will be referred to as a Marshall–Palmer (MP) distribution. Note that Marshall and Palmer give $N_0 = 8000\ \text{m}^{-3}\ \text{mm}^{-1}$ and $\Lambda = 41\ R^{-0.21}$. In fact, N_0 is known to vary considerably (Waldvogel 1974). Data from this experiment confirm this observation.

It is also known that the drop size distribution is not exponential as D goes to zero. In other words, there is a minimum D. For calculation of higher moments of the drop size distribution, this truncation is not a large error (Willis 1984). However, it clearly does not describe the distribution for smaller drop sizes. Often a distinctive peak is present in the drop size distribution (modal distribution). Consequently, another widely used parameterization of drop size distribution is the gamma distribution (Ulbrich 1983) given by

$$N(D) = N_G D^{\mu} e^{-\Lambda D}, \tag{3}$$

where μ is a shape parameter having both positive or negative values. In this expression, the units of N_G include μ ($\text{m}^{-3-\mu}\,\text{mm}^{-1}$) and are difficult to interpret physically.

If either Eq. (2) or (3) are assumed to describe the drop size distribution, then they can be combined with Eq. (1) to allow the parameters N_0, N_G, Λ, and μ to be estimated from measurements of the moments of the drop size distribution. For example (from Willis 1984), if the drop size distribution is assumed to be of the form given by Eq. (2) (MP), then liquid water content,

$$M = \frac{1}{6}\pi\rho_w \int D^3 N(D)\, dD \tag{4}$$

and reflectivity,

$$Z = \int D^6 N(D)\, dD \tag{5}$$

(both measurable quantities), can be used to estimate

$$\Lambda = \left(\frac{720}{\pi}\right)^{1/3}\left(\frac{M}{Z}\right)^{1/3} \tag{6}$$

and

$$N_0 = \Lambda^4\left(\frac{M}{\pi}\right). \tag{7}$$

In this experiment, M and Z can be calculated directly from the disdrometer data. Thus, estimates of N_0 and Λ can be calculated for each disdrometer data sample. In other words, a MP distribution can be ''fit'' to each data sample, even if the MP distribution is not appropriate. Even given the possibility that a MP distribution is not appropriate to a particular sample of rain, the parameter N_0 calculated using Eq. (7) proved useful at describing the different rainfall types.

The algebra associated with combining Eq. (3) into Eq. (1) is more complicated (Ulbrich 1983) and gives

$$\zeta = \frac{M_4^2}{M_2 M_6} \tag{8}$$

$$\mu = \frac{11\zeta - 7 - (\zeta^2 + 14\zeta + 1)^{1/2}}{2(\zeta - 1)} \tag{9}$$

$$D_0 = (3.67 + \mu)\left[\frac{\frac{M_4}{M_2}}{(4 + \mu)(3 + \mu)}\right]^{1/2} \tag{10}$$

$$\Lambda = \frac{(3.67 + \mu)}{D_0} \tag{11}$$

$$N_G = M_4 \Lambda^{\mu+5} \Gamma(\mu + 5), \tag{12}$$

where M_x indicates a moment of the drop size distribution (2nd, 4th, and 6th) and D_0 is another commonly used descriptor of the drop distribution, namely the median drop size by volume. Again, the disdrometer can be used to calculate the moments of the drop size distribution for each data point. Once again, these equations [Eqs. (8)–(12)] ''fit'' a gamma distribution to the observed data whether or not such a distribution is appropriate to a particular sample of rain. All of these parameters can be monitored for each rainfall event. The one that appeared most useful at discriminating the various ''types'' of rain was D_0.

One additional error associated with these drop size distribution parameters is truncation effects associated with Eq. (1). The algebra leading to Eqs. (8)–(12) assumes that the integration in Eq. (1) is from 0 to ∞, while the actual drop size limits are the minimum drop size detected by the disdrometer and the largest drop size actually present in the rain. An analysis of truncation effects is presented in Willis (1984) and Ulbrich (1985).

In order to try to identify features of the rainfall drop size distribution that affected the performance of the various rain gauges deployed in the experiment, each of the rain parameters described above were monitored for each event. In addition, total rainfall rate R, reflectivity Z, total drop flux N_f (m^{-2} s^{-1}), and median drop size D_0, calculated directly from the disdrometer data, were also monitored. The most useful descriptors were R, D_0, and N_0. The influence of wind speed U was also monitored.

3. Experimental setup

a. The AOML rain gauge facility

The AOML Rain Gauge Facility is located on Virginia Key, Miami, Florida. The rain gauges in the AOML Rain Gauge Facility include: 1) a weighing rain gauge, 2) a RM Young Model 50202 capacitance rain gauge, 3) several Scientific Technologies (ScTI) ORG-105 optical rain gauges, 4) a Belfort Model 382 tipping bucket rain gauge, 5) a Distromet RD-69 disdrometer, and 6) an acoustical rainfall system. All rain gauges were within 50 m of each other. The capacitance, optical, and tipping bucket rain gauges were within 5 m of each other. A more complete technical description of the facility and each rain gauge is found in Nystuen et al. (1996). A brief review is included here to give the reader a feel for the characteristics of the rain gauge instruments involved and the types of error that are to be expected for each gauge.

b. Description of the rain gauges

1) WEIGHING RAIN GAUGE

The weighing rain gauge operates on the principle of weighing the rainwater collected by the instrument. The measurement of rainfall rate is the difference in rainwater accumulation over a given time interval. The accuracy of the rainfall rate measurement is controlled by the precision of the water accumulation measurement, the rate at which rainwater drains from the catchment basin into the measurement chamber and the sampling interval. Technical difficulties with the automatic drainage system in the AOML instrument resulted in loss of data during several major events.

2) RM YOUNG CAPACITANCE RAIN GAUGE

The capacitance rain gauge is a collection-type gauge that was developed for potential use on buoys at sea (Holmes et al. 1981; Holmes and Michelena 1983). A probe consisting of a stainless steel rod covered by a teflon sheath is set inside a cylindrical collection chamber. The water surrounding this probe forms the outer ''plate'' of a coaxial-type capacitor, while the metal rod forms the inner ''plate.'' As the water height in the collection chamber rises, the surface area of the capacitor increases, increasing the capacitance. The capacitance is measured and converted to water height in the collection chamber. As with the weighing rain gauge, the measurement of rainfall rate is the difference in rainwater accumulation over a given time interval.

3) BELFORT TIPPING BUCKET RAIN GAUGE

Tipping bucket rain gauges measure rainfall by allowing rainwater to drain into a bucket that tips and drains after a given amount of rainwater has been collected. Each tip triggers a magnetic switch that sends a signal to a recording device. These instruments are widely used in automatically recording hydrographic arrays on land. This type of rain gauge is unsuitable for deployment at sea.

4) SCTI OPTICAL RAIN GAUGES

Unlike the previous three rain gauges, this instrument provides a measure of rainfall rate rather than accu-

TABLE 1. Acoustic raindrop sizes. The raindrop sizes are identified by different physical mechanisms associated with the drop splashes (Medwin et al. 1992; Nystuen 1996). These definitions for raindrop sizes will be used throughout this paper.

Drop size	Diameter (mm)	Sound source	Frequency range (KHz)
Tiny	<0.8	Silent	
Small	0.8–1.2	Loud bubble	13–25
Medium	1.2–2.0	Weak impact	1–30
Large	2.0–3.5	Impact	1–35
		loud bubbles	2–35
Very large	>3.5	Loud impact	1–50
		loud bubbles	1–50

mulation. Optical rain gauges measure the scintillation in an optical beam produced by the shadows of raindrops falling between a light source (a light emitting diode, or LED) and an optical receiver (Wang and Clifford 1975; Wang et al. 1977, 1978). The light intensity variation due to the shadow of a given drop is a function of drop size, fall velocity, optical geometry, and coherence of the LED light source. By choosing the proper geometry, the intensity variation caused by natural raindrops is proportional to rainfall rate (Wang et al. 1978).

5) JOSS–WALDVOGEL DISDROMETER

A disdrometer (Joss and Waldvogel 1967, 1969) is designed to measure the actual drop size distribution within rain by converting the momentum of individual raindrops striking the sensor head into an electronic signal proportional to drop size. The actual relationship depends on the characteristics of the sensor head. As each raindrop hits the sensor surface, the momentum of the impact is translated into an electrical pulse proportional to drop size.

6) ACOUSTICAL RAINFALL MEASUREMENT SYSTEM

Acoustical rainfall measurement uses the naturally occurring underwater sound produced by raindrops to quantitatively measure the rain (Nystuen 1996). Rainfall produces a unique underwater acoustic signal easily distinguished from other common sound sources (breaking waves, biology, etc.) and, furthermore, the sound levels produced by rain are much louder, by orders of magnitude, than these other sources. Acoustic signatures for different individual raindrop sizes have been identified (Medwin et al. 1992; Nystuen and Medwin 1995; Nystuen 1996) and are summarized in Table 1. Because the sound signature for each drop size range is unique, it is possible to invert the underwater sound field to estimate the drop size distribution within the rain (Nystuen 1996). Estimates of drop size distributions can then be used to estimate rainfall rate or other rain parameters, for example, reflectivity or liquid water content.

c. Description of the data

The experimental site is located at AOML on Virginia Key at 25.7°N, 80.1°W, an island several miles off the southeastern Florida coast within the city of Miami, Florida. Although the climate is subtropical most of the year, several distinctive climatological regimes are present. During the winter months, rainfall rates tend to be light, on the order of 2 mm h^{-1}. This is rainfall mostly associated with continental midlatitude frontal systems. During the spring transition months (April–June), several very intense rainfall events with extremely high rainfall rates occurred. During the rainy season (August–October), the rainfall events were mostly locally generated convective systems, including a few mesoscale convective systems (MCS) typical of rainfall in many tropical locations. Finally, a tropical storm can impact the area. One, Tropical Storm (TS) Gordon, occurred during the experiment (November 94).

Wind speeds at the experiment site were relatively low, less than 2 m s^{-1} most of the time. This was largely due to the sheltering mangrove trees. Nevertheless, mean wind direction and speed help to define the seasons. The mean wind direction was southerly during the winter. From April–October it was low and from the northeast. Tropical Storm Gordon produced relatively high mean winds.

The AOML rain gauge facility was operational from September 1993 until the end of January 1995 (17 months). During this period over 800 rain events occurred. A rain event was defined as any precipitation period with a rainfall rate over 1 mm h^{-1} and lasting at least 5 min. The automatic trigger for recording an event was the signal from one of the optical rain gauges. Whenever this signal indicated at least 1 mm h^{-1} rainfall, the system turned on. The system automatically resumed ''rest'' mode 5 min after the signal from the optical rain gauge dropped below 1 mm h^{-1} (and stayed below 1 mm h^{-1}). Thus, the minimum event length was 5 min. The data were subjectively examined to eliminate events with spurious or minimal triggers.

The temporal resolution of the distrometer was 1 min. Since data from the disdrometer were used to calculate descriptors of rainfall (N_0, D_0, etc.), the temporal resolution of data from the other instruments was set to a 1-min rainfall rate. Over 9000 min of 1-min rainfall data points are considered.

d. Examples of different rain events

(Events will be identified by Julian Day and start time (Local Standard Time). Thus, ''JD 032 @ 1747'' refers to the rain event that started at 1747 on 1 February.)

1) WINTERTIME EVENTS

February 1994 was a winter month during which very different types of events were recorded including the

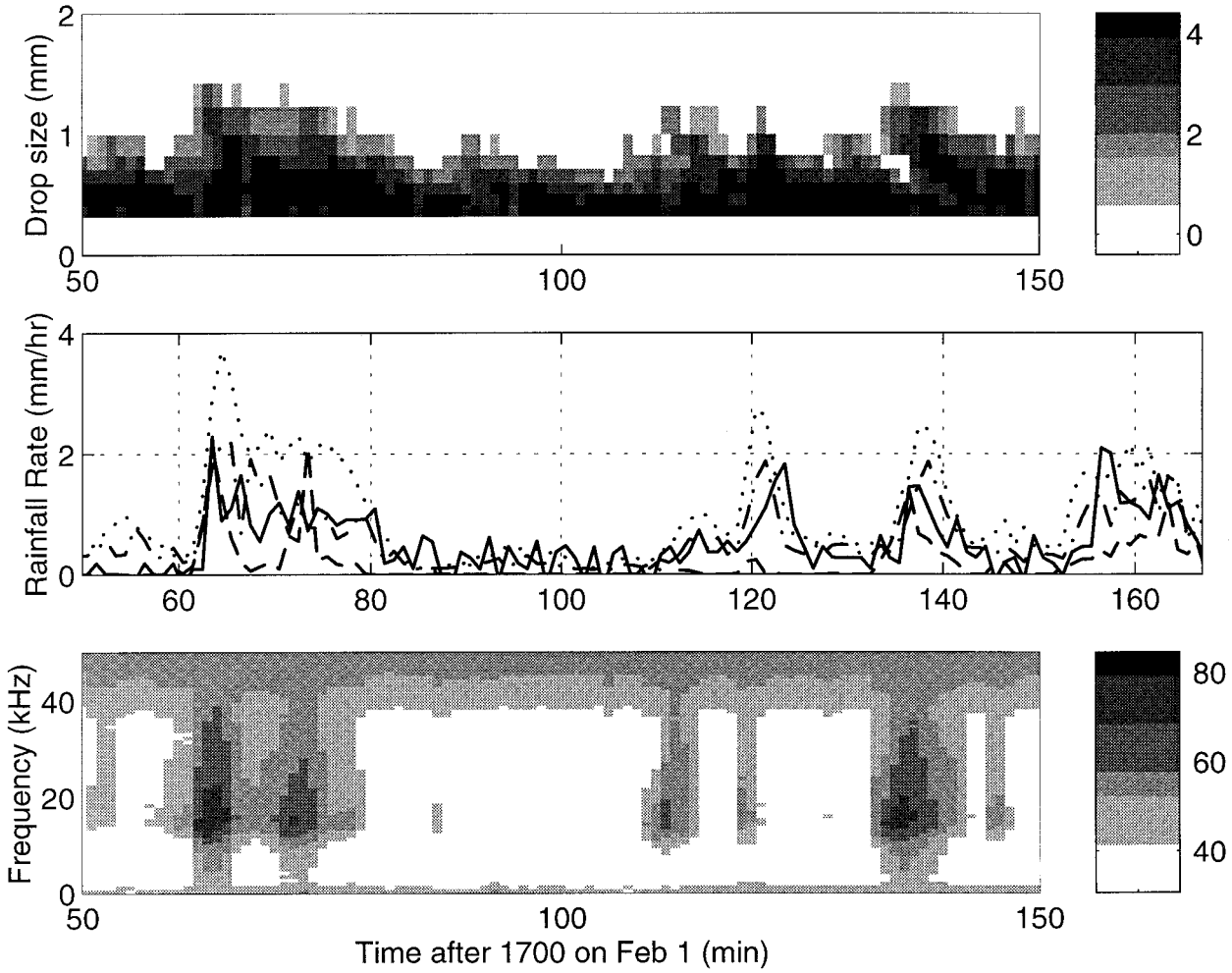

FIG. 1. The drop size distribution (upper panel) and the underwater sound field (lower panel) for event 032 at 1747 (1 Feb 1994). The units for the drop size distribution are 10^x m^{-2} s^{-1} mm^{-1}, where x is shown on the grayscale bar. The units for the sound field are shown in decibels (dB) relative to 1 μPa^2 Hz^{-1}. The middle panel shows the rainfall rate estimates from four of the rain gauges: capacitance (solid), optical (dotted), acoustic (dashed), and disdrometer (dash-dot).

longest continuous events of the entire experiment. These long events had light to moderate rainfall rates and relatively unchanging drop size distributions. One event, JD 032 @ 1747 (Fig. 1), was unique in that the median drop size D_0 was very small (0.5 mm) and N_0 was very high (over 10^5 m^{-3} mm^{-1}). The drop size distribution shows that the rain contained only tiny and small raindrops. The resulting Z–R relationship ($Z = 54R^{1.23}$), used to convert radar reflectivity (Z) into rainfall rate (R), has an unusually low value for α, the coefficient on R ($Z = \alpha R^{\beta}$). Figure 1 also shows the underwater ambient sound field. When the rain contains only tiny drops (<0.8-mm diameter), the sound field is at the ambient background of the pond. In other words, the tiny drops do not produce detectable sound underwater. Whenever small drops are present (0.8–1.2-mm diameter), sound is detected, especially in the 13–20 kHz band. Other examples of steady, light rainfall rate events showed much lower values of N_0 (order 5000) and larger values for D_0 (1–1.5 mm).

2) SPRINGTIME EVENTS (APRIL AND MAY 1994)

The events with the most intense rainfall rates occurred during these springtime months. During April, over 30 min of rainfall exceeding 100 mm h^{-1} occurred. One of these extreme rainfall events occurred on JD 150 (30 May). This event exhibited extreme jumps in N_0, D_0, N_f, and R (Fig. 2). The ambient sound and drop size distribution records are shown in Fig. 3. Five distinctive regimes are present. Initially (from min 13 to min 25), light rain was falling with very low N_0 and moderately high D_0. At this time, the rainfall rates are light (<2 mm h^{-1}), with the optical rain gauge relatively low compared to the other rain gauges. At min 26, the rainfall rate increased to moderate, N_0 ''jumped'' to a

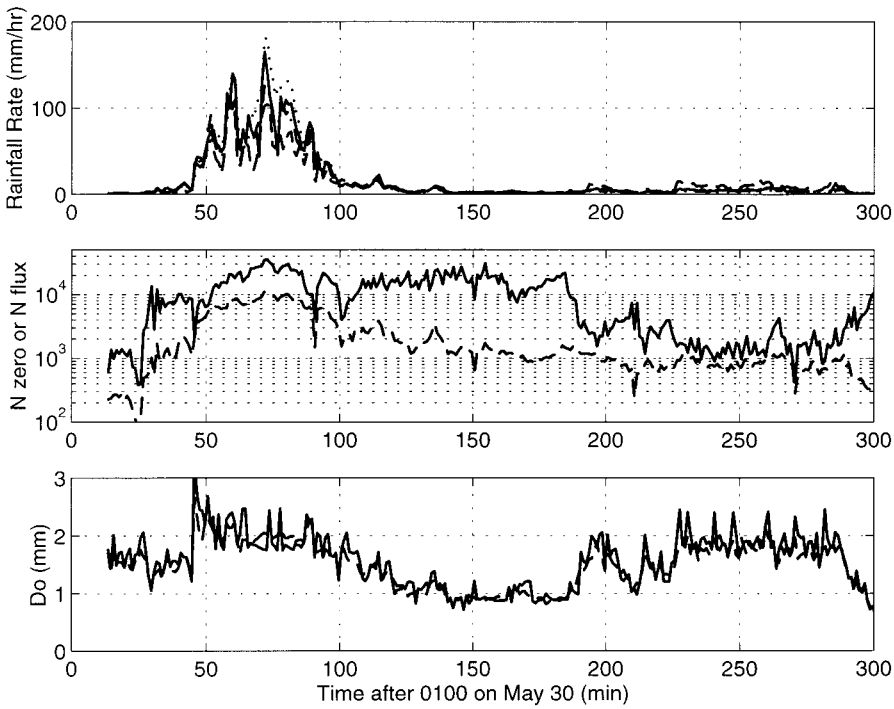

FIG. 2. Rainfall rate measurements and drop distribution parameters for event 150 at 0113 (30 May 1994). Top panel: Rainfall rate as measured by the disdrometer (dash-dot), capacitance gauge (solid), optical gauge (dotted), and acoustic sensor (dashed). Middle panel: N_0 (solid line), the coefficient for Eq. (2); N_f (dashed line), the total drop flux measured directly by the disdrometer (m^{-2} s^{-1}). Bottom panel: D_0, the median drop size by volume using Eq. (10) (dashed line) and measured directly by the disdrometer (solid line).

fairly high value, and D_0 decreased slightly. All of the rain gauges agree. The downpour starts at min 45 and lasts until min 100, with rainfall rates over 100 mm h^{-1}. Here, N_0, D_0, and N_f are all high. The underwater sound field is very loud and relatively uniform across the entire frequency band. No peak in the frequency range from 13–20 kHz is apparent. The sound generated by small raindrops in this range is either suppressed or overwhelmed by the sound produced by the large and very large raindrops present in the rain at this time. During the most intense rain (min 70–85), the optical rain gauge is high relative to the other gauges and the disdrometer and tipping bucket gauges are low relative to the weighing and capacitance gauges, the two collection-type gauges. At min 100, the heaviest rainfall ends: N_f and D_0 drop in value; however, N_0 does not drop. The rainfall rate is light during this interval; the sound field is dominated by the 13–25 kHz sound produced by small (0.8–1.2 mm) drops. This is the remarkably loud ''sound of drizzle.'' Few large (2.0–3.5 mm) or very large (>3.5 mm) drops are present. The rainfall rates from all of the rain gauges agree. At min 200, the rain begins to contain large and very large raindrops. Whenever large drops are present, the sound field below 10 kHz increases in intensity, indicating acoustic detection of these larger raindrops. During this period, N_0 jumps to a relatively low value and D_0 jumps to a relatively large value. The optical rain gauge measures lower rainfall rates than the other rain gauges; the acoustic rain gauge is high.

The five intervals just described are cleanly separated on a *Z–R* diagram (Fig. 4). The three groups with high N_0 (min 25–44, min 45–100, min 101–180) fall on the ''convective'' rainfall line described by Tokay and Short (1996) ($Z = 139R^{1.43}$). The low N_0 periods (min 13–24, min 200–300) are closer to the Tokay and Short ''stratiform'' *Z–R* relationship ($Z = 367R^{1.30}$). Classification of the min 101–180 period as convective is questionable. Another presentation of the data from this event is Fig. 5 showing moments (2nd, 4th, and 6th) of the drop size distribution and the sound field at four frequencies (2, 5, 15, and 40 kHz). The sound levels at 2 and 5 kHz are highly correlated to M_6, $r = 0.97$ and $r = 0.96$, respectively, as both the lower frequency sound field and reflectivity ($Z = M_6$) are very sensitive to the presence of larger raindrops (>2.0-mm diameter). Between min 100 and min 180, the larger drops are generally absent; however, small drops are present throughout this period. During this time, the sound field changes dramatically, with the sound intensities at lower frequencies dropping, but not at 15 kHz, the center of the band where small raindrops produce their underwater sound. Earlier, during the downpour (min 45–85), the sound levels are very high. The elevated sound level at 40 kHz (over 60

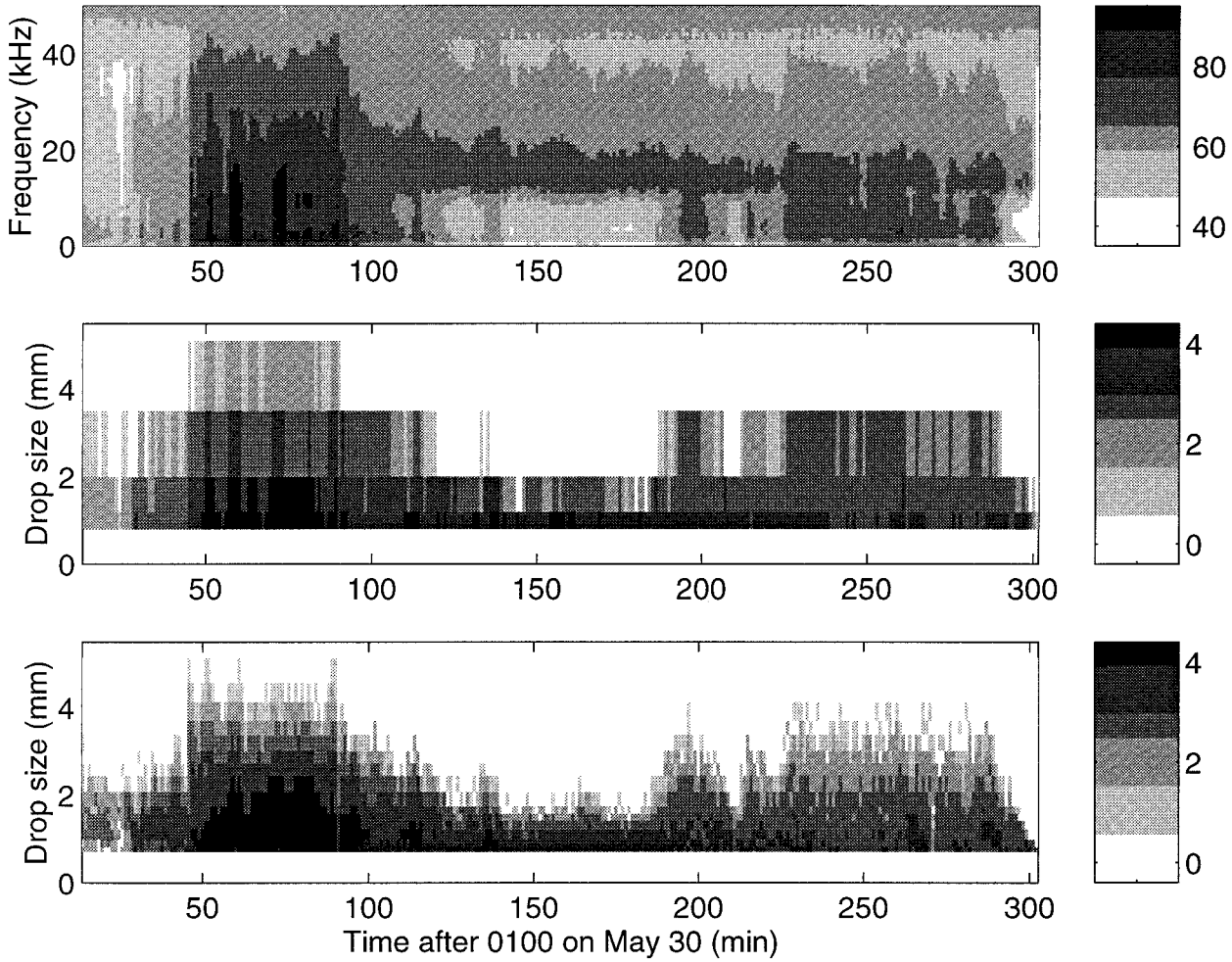

FIG. 3. The drop size distribution (upper panel) and the underwater sound (upper panel) and drop size distributions using the acoustic inversion (middle panel) and the disdrometer (lower panel) for event 150 at 0113 (30 May 1994). The units for the sound field are shown in decibels (dB) relative to 1 μPa^2 Hz^{-1}. The units for the drop size distribution are 10^x m^{-2} s^{-1} mm^{-1}, where x is shown on the grayscale bar.

dB relative to 1 μPa^2 Hz^{-1}) is a reliable indicator for extremely large raindrops (over 3.5-mm diameter).

3) SUMMERTIME EVENTS

The summertime rain events were generally smaller, shorter duration convective events showing many of the features previously described. There were a couple of short events with very irregular drop size distributions. One example is from JD 188 (7 July; Fig. 6). Clearly MP or gamma distributions are inappropriate for this example. Of course, the parameterizations such as MP or gamma are intended for ''mean'' conditions, not individual, unusual events such as this example. Here, N_0 is extremely low ($<10^3$) and D_0 is extremely large (>3 mm). The optical rain gauge rainfall rate is low relative to the other gauges and the acoustical measurement is high. The Z–R relationship for this event is $Z = 2188R^{1.24}$. The α coefficient on R ($Z = \alpha R^{\beta}$) is an order of magnitude larger than most published values, which, of course, are typically long temporal averages for mean conditions (Ulbrich 1983).

4) FALL CONDITIONS—MESOSCALE CONVECTIVE SYSTEMS

September and October of both years were relatively rainy months. Most of the events can be described as mesoscale convective systems (Houze 1989). These systems are typical of tropical regions. They include both convective and stratiform components, and can often last for hours. The characteristics of the rainfall are similar to previously described examples. During the convective portion of the events, N_0, N_f, and D_0 show a lot of variability. During the first few moments, N_0 and N_f are often low, while D_0 is high. During the most intense portion of the event, when R can exceed 100 mm h^{-1}, N_0 is of order 20 000 and D_0 is roughly 2 mm.

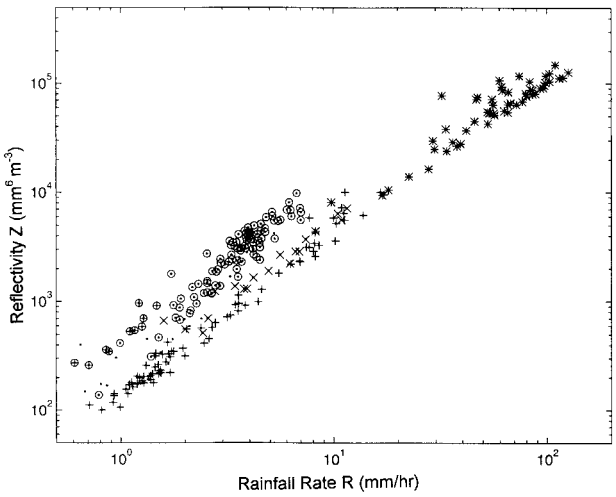

FIG. 4. The *Z–R* (reflectivity–rainfall rate) relationship for event 150 at 0113 (30 May 1994). Different periods of the event are marked with different symbols: Mins 13–24 "⊕"; Mins 25–44 "×"; Mins 45–100 "*"; Mins 101–180 "+" and Mins 200–300 "⊙."

During this interval, the disdrometer and tipping bucket report rainfall rates that are low relative to the other gauges, the optical gauge is relatively high, while the capacitance and weighing gauges are intermediate. In contrast, during the stratiform portion of the events, N_0 has a relatively steady and low value, of an order of 2000–3000, and a moderate and steady value of D_0, of an order of 1.5 mm This is typical of MCS stratiform rain. The rainfall rates are moderate (e.g., 2–5 mm h^{-1}), with the optical gauge reporting relatively low rainfall rates and the acoustical rain gauge relatively high.

5) TROPICAL STORM GORDON (NOVEMBER 1994)

Tropical Storm Gordon lashed Miami for a couple of days (14–16 November). This provided data with relatively high winds. The character of the rain events were different than during the other months of the experiment. The events showed rapid variability in time, with all variables changing on a time scale of a few minutes. This was the prominent feature of rain events during TS Gordon. The acoustical measurements of rainfall rate were relatively low during TS Gordon, suggesting that wind speed, which was relatively high, reduces sound production by raindrops, especially small raindrops.

4. Rain gauge evaluations

a. Overview

In order to evaluate the performance of a rain gauge, one must identify the "true" rainfall rate. This, of course, is unknown. However, six different rain gauges are present in the Miami rain gauge network, and so it is possible to compare the relative performance of one gauge to the mean of all gauges or to some subset of

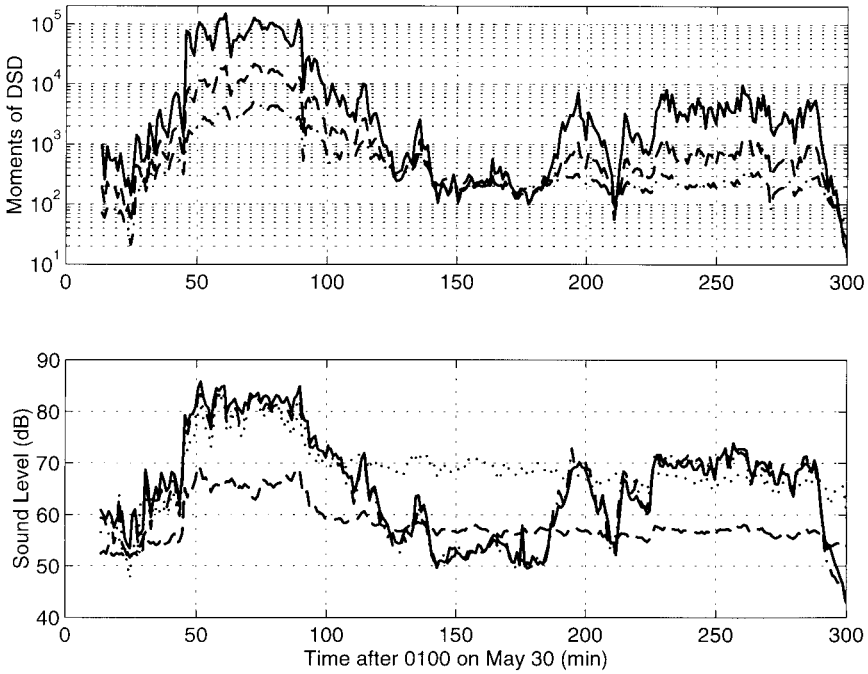

FIG. 5. Measured moments of the drop size distribution (upper panel) from the disdrometer. Shown are M_2 (solid line), M_4 (dashed line), and M_6 (solid line). The units are mm^x m^{-3}, where x is the moment (2nd, 4th, or 6th). The bottom panel shows the sound level at four selected frequencies: 2 kHz (solid), 5 kHz (dash-dot), 15 kHz (dotted), and 40 kHz (dashed). The units are dB relative to 1 μPa^2 Hz^{-1}.

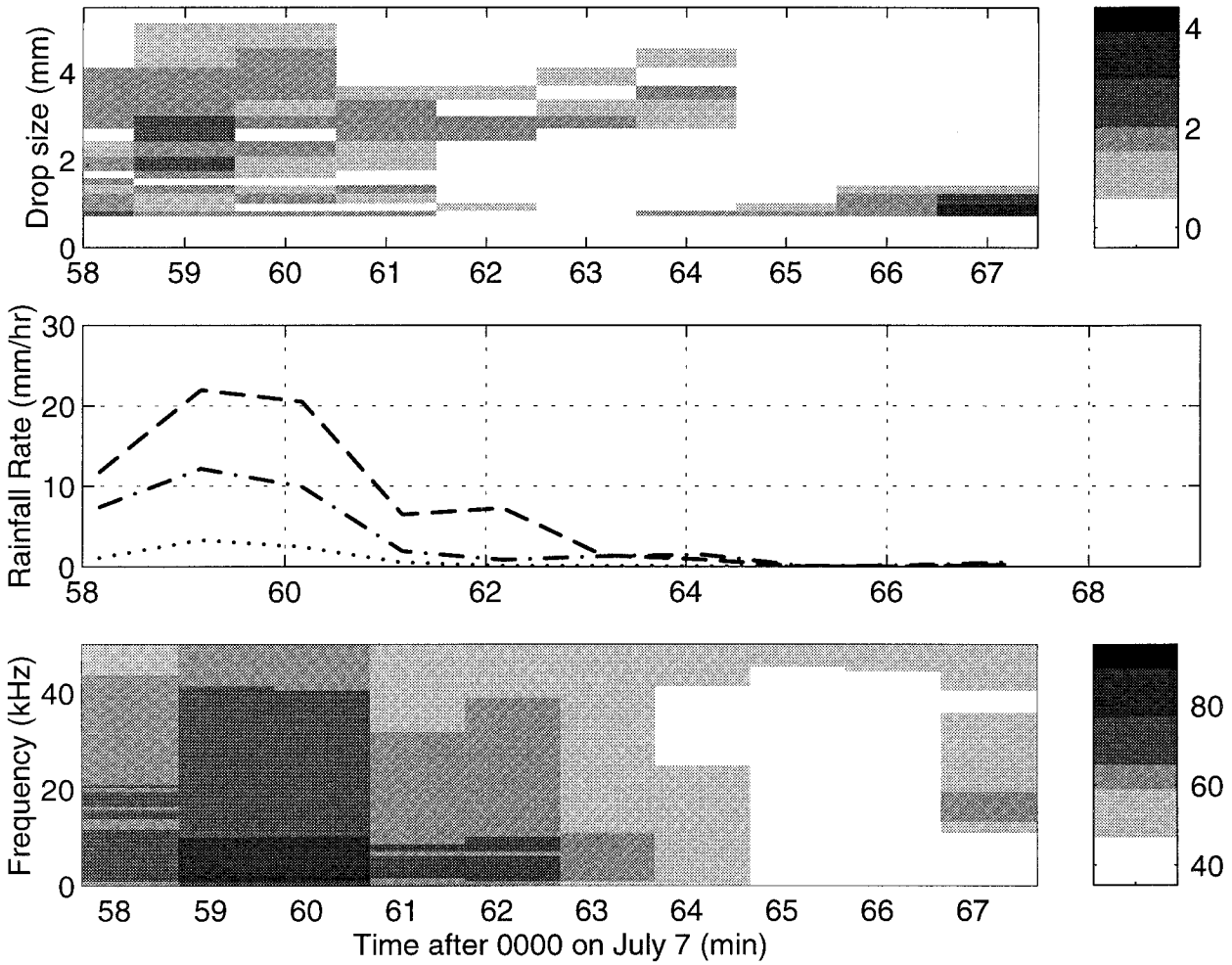

FIG. 6. The drop size distribution (upper panel), underwater sound (lower panel) and measured rainfall rates (middle panel) for event 188 at 0057 (7 Jul 1994). The units for the drop size distribution are 10^x m^{-2} s^{-1} mm^{-1}, where x is shown on the grayscale bar. The rainfall rate (mm hr^{-1}) measurements shown are: the disdrometer (dash-dot), optical (dotted), and acoustic (dashed). The units for the sound field are shown in decibels (dB) relative to 1 μPa^2 Hz^{-1}.

rain gauges. Using a subset of the rain gauges is appropriate as some of the rain gauges performed, or failed to perform, in ways that meant if their data were to be included in a mean rainfall rate then their performance characteristics would become part of the evaluation of the other gauges. For example, if one gauge is always higher than the true rainfall rate, then by including its measurement in the mean, all other gauges, even if correct, would be lower than the mean. Subjective observation of the rain gauge performances suggested that the weighing, acoustic, and tipping bucket rain gauges should be excluded from the mean. The weighing gauge was not used as it failed during several of the main events, apparently because the automatic drainage system failed. These events, of course, were the most important events in terms of accumulation and extremely high rainfall rates. The acoustic rain gauge is not used as it shows high scatter compared to the other gauges. This variance would ''contaminate'' the statistics of the other gauges if included in the mean. The tipping bucket rain gauge was also not used as its one minute rainfall rate resolution is ± 12 mm h^{-1}. Including it in the mean contaminated the statistics of the other rain gauges at low and moderate rainfall rates (<5 mm h^{-1}).

Conversely, by excluding selected rain gauges from the mean, there is a statistical bias in favor of the remaining gauges. Because their own data is part of the mean, and there is a perfect correlation to one's own data, the correlation to the mean will be higher than if no data from that particular rain gauge were used to form the mean. A rain gauge not used as part of the mean will not have this advantage. Thus, we should expect the statistics to ''favor'' the capacitance, optical, and disdrometer rain gauges. This ''favoritism'' is justified as, subjectively, the mean of these three gauges is thought to be closest to the true rainfall rate.

Table 2 shows the first-order correlation coefficients for 1-min rainfall rates between the various rain gauges

TABLE 2. First-order correlation coefficients of one minute rainfall rates between the various rain gauges for selected months during the experiment.

Month:	Oct 93	Feb 94	Apr 94	May 94	Jul 94	Sep 94	Gordon	Dec 94	Jan 95
Number of minutes of rain	878	1287	1237	423	574	1460	1676	908	659
Gauge									
Disdrometer[a]	0.94	0.91	0.98	0.97	0.94	0.90	0.95	0.96	0.98
Acoustic[b]	0.85	0.84	0.92	0.92	0.89	0.93	0.95	0.87	0.92
Optical[c]	0.97	0.92	0.97	0.97	0.96	0.98	0.96	0.92	0.98
Capacitance[d]	0.92	0.92	0.97	0.97	0.93	0.93	0.94	0.92	0.97
Weighing[b]	—	—	—	0.99	0.98	0.96	—	0.84	0.99
Tipping bucket[b]	0.96	0.81	0.98	0.98	0.94	0.96	0.95	0.93	0.92

[a] Correlation between the disdrometer rainfall rate and the optical rain gauge.
[b] Correlation with respect to the mean of the disdrometer, optical, and capacitance rain gauges.
[c] Correlation between the optical and capacitance rain gauges.
[d] Correlation between the disdrometer rainfall rate and the capacitance rain gauge.

for selected months of the experiment. These months were chosen to sample all of the rainfall ''seasons'' including TS Gordon. With the exception of a few months when the weighing rain gauge failed during major rain events, all of the gauges are highly correlated with one another. The lowest correlations coefficients occurred in February 1994 (0.81–0.92). This was a month with extremely variable rainfall types, including long duration drizzles/light rains and short events with extremely large raindrops and highly irregular drop size distributions. In contrast, during TS Gordon, the drop size distribution shapes were remarkably similar (Marshall–Palmer type) and the correlation coefficients are uniformly high (0.94–0.96). One subset of the rainfall dataset that had much lower correlation coefficients for two of the rain gauges was light rainfall, with mean rainfall rates of less than 2 mm h^{-1}. In this circumstance the correlation coefficients between the disdrometer rainfall rate and the capacitance gauge ranged from 0.13 (during TS Gordon) to 0.65 (May 94) with a mean value of 0.36. This appeared to be due to noise in the capacitance gauge measurement. The other instrument that performed poorly during light rain was the tipping bucket rain gauge. Its correlation coefficients compared to the other gauges during light rain ranged from 0.09 to 0.18. It simply can not resolve light rainfall rates using a 1-min time interval.

Another measure of rain gauge performance is the first-order regression with respect to the other rain gauges. Table 3 shows the slopes of the first-order regression of the rain gauge 1-min rainfall rate values when compared to the mean of the disdrometer, capacitance, and optical rain gauges for selected months (subsets of the data) during the experiment. The slope of the regression gives the mean bias of each gauge and can be used to ''calibrate'' each sensor, if the mean is assumed to be the true rainfall rate. The consistency of this number across the different subsets of data can be used as an indicator of reliability of performance for each gauge. The offset of the regression is also part of each rain gauge's bias. These first-order regression offset values are not explicitly presented as, in general, they were very small, usually less than 1 mm h^{-1}. Because their own data forms part of the mean, we should expect numbers from Table 3 to favor the disdrometer, capacitance, and optical rain gauges. Nevertheless, trends are apparent.

Two of the sensors, the disdrometer and the tipping bucket, tend to slightly underestimate rainfall rate: the mean regression slopes are 0.91 and 0.94, respectively.

TABLE 3. First-order regression slopes for various months during the experiment with respect to the mean of the 1-min disdrometer, capacitance, and optical rainfall rates.

Month:	Oct 93	Feb 94	Apr 94	May 94	Jul 94	Sep 94	Gordon	Dec 94	Jan 95
Number of minutes of rain	878	1287	1237	423	574	1460	1676	908	659
Gauge									
Disdrometer	0.92	0.93	0.88	0.87	0.98	0.91	0.88	0.96	0.88
Acoustic	0.95	1.65	1.07	0.76	1.11	0.71	0.55	0.69	1.00
Optical	1.12	0.97	1.17	1.15	0.97	1.09	1.13	1.07	1.07
Capacitance	0.96	1.07	0.95	0.97	1.05	0.99	0.99	0.97	1.05
Weighing	—	—	—	1.10	1.16	1.03	—	0.78	1.22
Tipping bucket	0.93	0.84	0.88	0.91	1.03	0.96	0.92	0.99	0.98

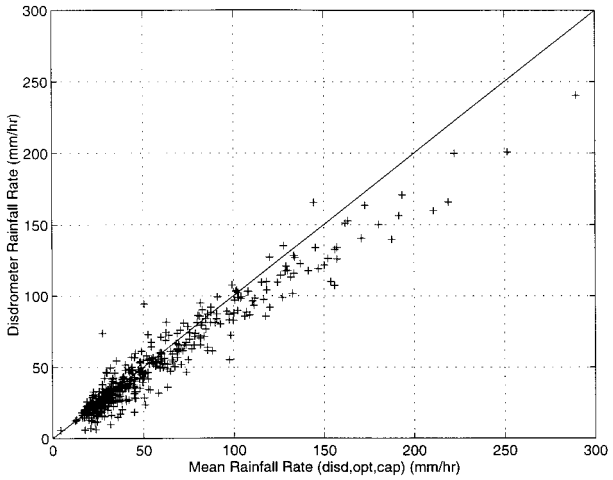

FIG. 7. Disdrometer rainfall rates compared to the mean of the disdrometer, capacitance, and optical rain gauges during heavy and extremely heavy rainfall. The data include 444 min of heavy rainfall from Apr, May, Sep, and TS Gordon.

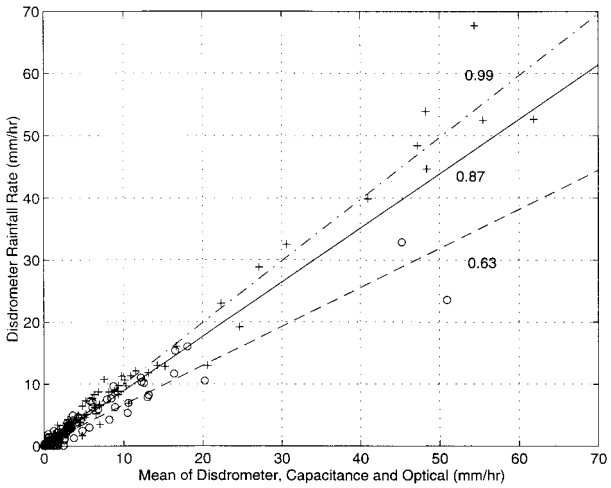

FIG. 8. Disdrometer rainfall rates compared to the mean of the disdrometer, capacitance and optical rain gauges for different wind speeds during TS Gordon. Three categories are shown: calm, <2 m s^{-1}, ''+'' symbol, dash-dot line; breezy, 2–5 m s^{-1}, solid line; and windy, >5 m s^{-1}, ''○'' symbol, dashed line. Individual data points for the breezy category are not shown. The slope of the first order regression is indicated next to each regression line.

In contrast, the optical rain gauge overestimated rainfall rate: mean slope of 1.08. And, by this measure, the capacitance rain gauge is closest to the mean rainfall rate as its mean regression slope is 1.00. The acoustic sensor did not show a mean trend, but rather a high variability—an indication of inconsistent performance. The mean regression slope for the acoustic sensor is 0.94, but the range is from 1.65 (February 1994) to 0.55 (TS Gordon). The high value in February 1994 is associated with overestimation of rainfall rate during a single rainfall event. If this event is removed from the data, then the slope of the regression becomes 1.03. Similarly, low slope values for other months are associated with single events where the acoustic gauge underestimated rainfall rate. However, in TS Gordon the low regression slope value is due to apparent low sound levels throughout the event, which resulted in low estimates for the small and medium raindrop populations.

b. The disdrometer

Table 3 shows that the disdrometer tended to underestimate the rainfall rate with respect to the other gauges by about 10%. The mean slope coefficient is 0.91. In four of the datasets considered, the slope is less than 0.9. Two of the these months (April and May 1994) were months with tens of minutes of extremely high, over 100 mm h^{-1}, rainfall rates. Figure 7 shows the disdrometer rainfall rates for 444 minutes when the rainfall rate was over 20 mm h^{-1}. When the rainfall rate is extremely high, over 100 mm h^{-1}, the disdrometer measurement is low relative to the optical and capacitance rain gauges. Several explanations are suggested.

First, the disdrometer has a self-noise control. When the ambient noise is louder, smaller drops are not counted. The noise floor is higher during extremely high rainfall rates, and so this is when the small drop count is suppressed. This is a design feature is built into the disdrometer to maximize the likelihood of detecting larger drops, which contain much more water and are therefore ''more important'' than the smaller drops. Extrapolating to include the ''missing'' small raindrops reduces, but does not eliminate, this underestimation relative to the other rain gauges.

Another explanation for underestimation during extremely high rainfall rates is that a finite time needed for the instrument to recover from a drop strike and be ready for the next drop. This time is not clearly identified by the manufacturer, however the need for a ''duty cycle'' correction is recognized (Sheppard and Joe 1994; Nystuen et al. 1994). A third possibility is that water accumulation on the sensor head may change its calibration, especially for drops directly striking pools or existing drips of water on the sensor head.

Another group of data showing a low bias for the disdrometer are the data from TS Gordon. These data included the windiest conditions of the experiment. Figure 8 shows the rainfall rate data from the disdrometer compared to the mean of the disdrometer, optical, and capacitance rain gauges for three different wind speed categories: calm, <2 m s^{-1}; breezy, 2–5 m s^{-1}; and windy, >5 m s^{-1}. As wind speed increases, the slope of the regression decreases. The trend was also present in the December 1994 data, although those data were less statistically significant. An examination of the drop distribution measured by the disdrometer during relatively windy events shows that the smallest drop categories have low drop counts. This could be an indication that the self-noise floor of the disdrometer is higher during windy conditions, suppressing the smallest drop

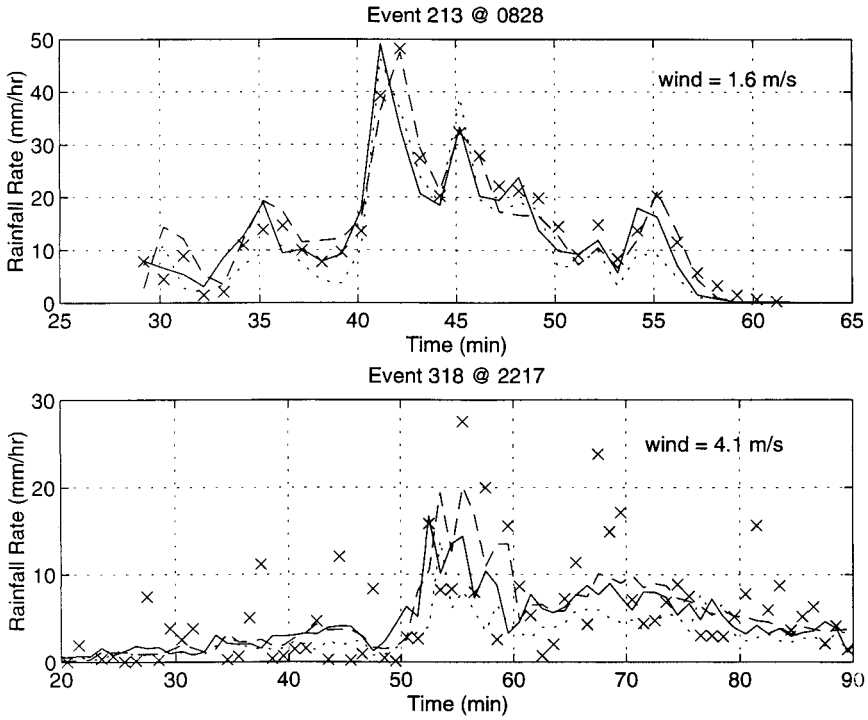

FIG. 9. The rainfall rate measured by the capacitance rain gauge, "×" symbol, compared to the disdrometer (solid line), optical (dashed line), and acoustic (dotted line) gauges. Two events are shown: event 213 at 0828 (1 Aug 1994) has low wind speed with good agreement between gauges, and event 318 at 2217 (14 Nov 1994) has relatively high wind speeds. Under the higher wind speed conditions the capacitance gauge exihibited more instrument noise.

categories. Or air flow over the sensor head may prevent the smaller drops from striking the sensor head and thus producing a reduced drop count. Again, neither of these explanations can fully account for the reduced rainfall rate relative to the other sensors as the tiniest drops do not represent enough of the total volume of rain water to make up the difference in rainfall rate. In fact, it may be that all drop categories are affected by the air flow across the sensor head. This air flow may reduce the vertical momentum transfer from single drop strikes causing an underestimation of the individual drop size for each raindrop. This, of course, would result in an underestimation of rainfall rate. If true, this means that disdrometers deployed on buoys or ships will tend to underestimate rainfall rate as exposure to wind is likely.

c. The capacitance rain gauge

The capacitance rain gauge performed quite consistently throughout the experiment. The slope of the regression, Table 3, shows no trends and has a mean value of 1.00. One problem with this gauge is instrument noise at the lower rainfall rates. In the light rain subset of the data, rainfall rate less than 2 mm h^{-1}, the correlation between the capacitance rain gauge and the other gauges was quite low. For example, during light rain the correlation coefficient between the disdrometer rainfall rate and the capacitance gauge ranged from 0.13 to 0.65, with a mean value of 0.36. The cause of this low correlation is "instrument noise" due to the rate of "dripping" from the catchment basin into the measurement reservoir (Nystuen et al. 1996). It can be reduced by increasing the averaging time from 1 min to a longer time interval.

Figure 9 shows another potential problem with this gauge. When the wind is higher, there is more scatter in the capacitance measurement when compared to the other rain gauges for moderate and heavy rainfall rates. The most likely influence of wind on the sensor would be to cause the instrument to vibrate. This should actually reduce the noise due to irregular dripping. Thus, the "noise" shown in Fig. 9 is more likely to be associated with motion of water within the measurement chamber itself. Rain gauge motion and vibration on buoys or ships may make this type of noise ubiquitous. Note that, for the event shown in Fig. 9, the accumulation total of the capacitance gauge over the whole event is in agreement with the optical and tipping bucket gauges. Thus, this noise is only associated with one minute rainfall rate measurements, rather than long time period accumulations.

There is no reason to expect that a collection-type rain gauge should be sensitive to changes in the drop size distribution. Indeed, no variations in performance

with respect to the other rain gauges were detected with changes N_0 or D_0, two of the drop size distribution parameters previously introduced. Under extremely heavy (over 100 mm h^{-1}) rainfall rate conditions, the rainfall rate measurement of the capacitance gauge was intermediate to the other gauges: the optical rain gauge was higher, the disdrometer and tipping bucket gauges were lower. Again, there is no reason to expect a collection-type gauge to be biased by extremely heavy rainfall rates, and so the ''correct'' rainfall rate during extremely heavy rainfall is probably close to the value measured by the capacitance gauge. In fact, when operating correctly, the extremely heavy rainfall rate measurements from the weighing rain gauge, another collection-type gauge, agreed with the capacitance rain gauge values.

d. The weighing gauge

With its large catchment basin and precision weight measurement, this gauge was expected to be the ''best'' rain gauge in the system. Unfortunately, the automatic siphoning system for this gauge failed to perform correctly, causing it to be unreliable. In particular, this gauge failed during long and high accumulation events, in other words, the most interesting events, throughout the experiment. The blank values in Tables 2 and 3 indicate months when significant loss of data occurred.

When this gauge was functional, the mean slope of the regression was about 1.02, a slight overestimation of rainfall rate compared to the other rain gauges. It did not show any trends with respect to the rainfall conditions considered. Under extremely high rainfall rates, its measurements agreed with the mean of the capacitance, disdrometer, and optical gauges. As expected, there was no trend with respect to parameters of the drop size distribution (rainfall type). Because of the need for a stable platform, the weighing gauge is not a candidate for buoy or ship deployment.

e. The tipping bucket

Another gauge that can not be deployed on buoys is the tipping bucket rain gauge. According to Table 3, it slightly underestimates rainfall rate. Low slope values were recorded in April and May, the months with the extremely high rainfall rates. Figure 10 shows the performance of this gauge during extremely heavy rainfall rates. The highest rainfall rates are being underestimated. It is thought that water loss between ''tips'' is responsible for this underestimation (e.g., Marselek 1981, and others). One month with very low slope value in Table 3 is February 1994. During this month the gauge failed to tip during several events. Biological interference is suspected. The slope is also low during TS Gordon. There is a trend in the data showing that as the wind speed increase, the slope of the regression decreases. This may be due to the interference of air flow

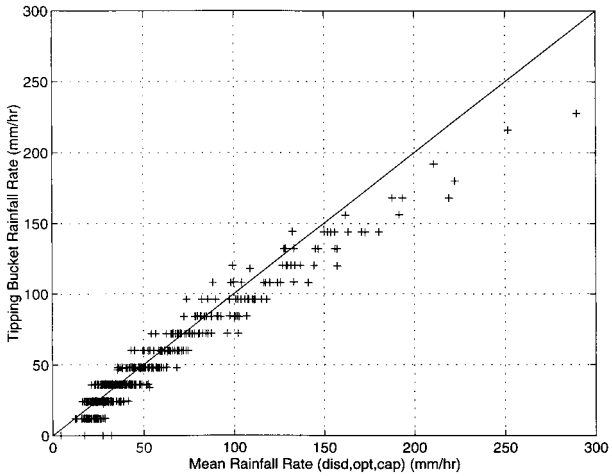

FIG. 10. Tipping bucket rain gauge rainfall rates compared to the mean of the disdrometer, capacitance, and optical rain gauges during heavy and extremely heavy rainfall. The data include 444 min of heavy rainfall from Apr, May, Sep, and TS Gordon.

over the catchment basin. Wind is known to reduce catchment in collection-type gauges (see e.g., Legates and deLiberty 1993) and standard corrections can be applied. This gauge has an 1-min rainfall rate resolution of ± 12 mm h^{-1}. Consequently, it is poorly correlated to the 1-min rainfall rate measurements as measured by the other rain gauges in the system when the rainfall rate is light (<2 mm h^{-1}) or moderate (2–5 mm h^{-1}). It simply can not measure light or moderate rainfall rates using an one minute time interval. Again, as expected, this gauge showed no trends with respect to changes in the drop size distribution parameters.

f. The optical rain gauge

Unlike the weighing, capacitance or tipping bucket rain gauges, the optical rain gauge makes a measure of rainfall rate rather than an accumulation. The physics of the measurement, a scintillation due to raindrop shadows, suggest that the measurement might be affected by changes in the shape of the drop size distribution. Indeed, it appears that changes in performance of the optical gauges are associated with variations in the parameters of the drop size distribution.

While Marshall and Palmer (1948) had initially suggested that N_0, the intercept value of an exponential drop size distribution [Eq. (2)] was a constant of about 8000 m^{-3} mm^{-1}, extreme values from less than 10^3 to over 10^5 were observed during this experiment. Although not strictly mathematically corrent, this parameter physically appears to describe the ratio of small drops to large drops within the rain. When the data are stratified by N_0, the bias of the optical rain gauge is proportional to N_0 (Fig. 11). Examples from section 3 can be used to identify the rain conditions when the optical rain gauge biases low or high.

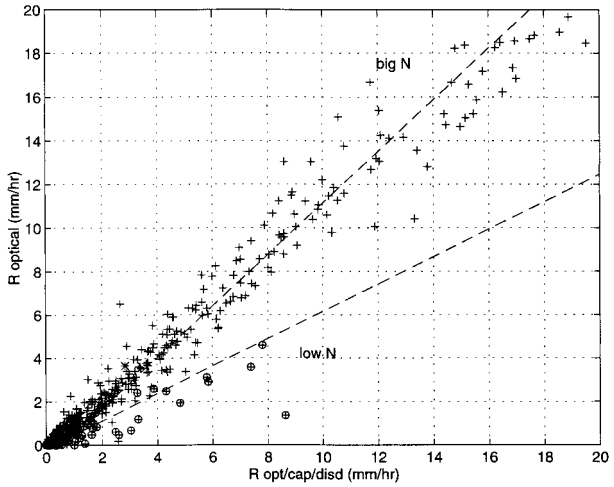

FIG. 11. Optical rain gauge performance as a function of N_0. The slope of the first-order regression is proportional to N_0. In this example, low N_0 values ($N_0 < 10^3$) are shown by the "⊕" symbols and dashed line (slope = 0.61) and high N_0 values ($N_0 > 10^4$) are shown by the "+" symbols and solid line (slope = 1.06). Intermediate data points ($10^3 < N_0 < 10^4$) are not shown.

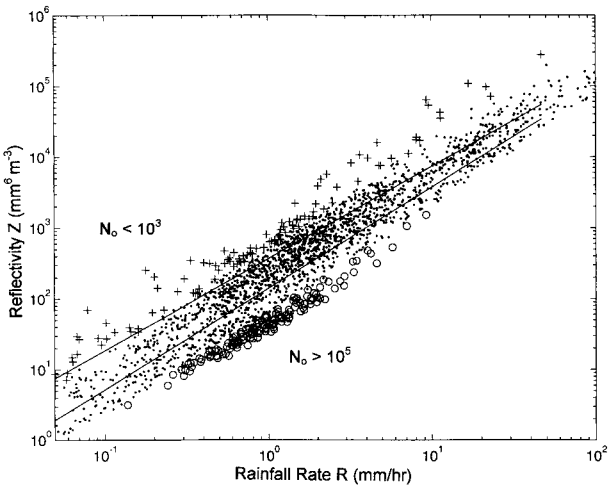

FIG. 12. The reflectivity–rainfall rate (Z–R) diagram stratified by N_0 values. Reflectivity is the integrated moment of the rain that a weather radar measures. Typically, empirical relationships are used to convert the radar reflectivity to rainfall rate. From this diagram, it is clear that N_0 is a parameter that can be used to describe the Z–R relationship. When N_0 is low, a given rainfall rate will be associated with a higher reflectivity than the same rainfall rate when N_0 is higher. In other words, using a fixed Z–R relationship, reflectivity (a radar) will overestimate rainfall rate when N_0 is low and underestimate rainfall rate when N_0 is high. This is opposite to the bias of the optical gauge and suggests that comparison of optical gauge data with radar data will be most difficult in rainfall situations where N_0 is variable. Two Z–R curves are shown in the figure: the upper one is the Tokay and Short (1996) stratiform Z–R relationship (relatively more large drops) and the lower curve is their convective Z–R relationship.

Low values of N_0 ($N_0 < 5000$) were observed under two general circumstances: when the rain contains relatively few drops, usually at the start or end of a rain event; and during some long duration light drizzles, in particular, the stratiform rain associated with mesoscale convective systems. The first situation includes the start of larger convective events, when large to very large drops are often present and the rainfall rate can reach tens of millimeters per hour. Examples include events 150 or 188 (Figs. 2 and 6, respectively). The rain parameter D_0, the median drop size [Eq. (10)], can be moderate (of order 1.7 mm at the beginning of event 150: mins 15–25) to extremely large (over 3 mm in event 188). The rainfall rate data show that the optical gauge is low relative to the other rain gauges at these times (Figs. 2 and 6, respectively). The other rain situation when the optical rain gauge rainfall rate was low relative to the other gauges was during stratiform drizzle associated with mesoscale convective systems. One example includes event 150, mins 230–270 (Fig. 2). The D_0 values were moderate (1.8 mm).

High values of N_0 ($N_0 > 20\,000$) were observed under two circumstances: light rain with only tiny or small drops, in particular event 032 (Fig. 1); and during extremely heavy rainfall with very high total drop counts. Under both of these conditions, the rainfall rate recorded by the optical rain gauge was high relative to the other rain gauges. In the light rain example (Fig. 1), D_0 is very low (order 0.5 mm) and N_0 is extremely large (order 10^5). Specific examples of the high bias during extremely heavy rainfall can be found in event 150 (Fig. 2, mins 50–90). Here, N_0 exceeds 20 000; D_0 is roughly 2.0 mm, a fairly large value; and the total drop count, N_f, is very large (order 10 000).

Intermediate values of N_0 (5000–20 000) generally resulted in agreement between the optical gauge and the other gauges. Examples include moderate rain periods of event 150 (Fig. 2, mins 30–45 or mins 130–180). In these events, D_0 ranged from a relatively low value of 1 mm to a relatively large value of 2 mm.

Thus, N_0 appears to be an indicator for the performance of the optical gauge. When the rain contains relatively few, but larger drops, N_0 is often low and the optical gauge rainfall rate is low relative to the other sensors. Event 188 is an extreme example of this situation. On the other hand, if the rain contains relatively more tiny drops, as suggested by a high value of N_0, then the optical gauge is relatively high. This includes rainfall rates from light drizzle (event 032) to extremely heavy downpours (events 150, etc.), with D_0 varying from small to large. This result is consistent with the finding of Nystuen et al. (1996) that the optical gauge rainfall rate is more highly correlated to a lower moment of the drop size distribution than rainfall rate (the 3.6th moment). It is also a bias, which is opposite to that of a weather radar (Fig. 12), suggesting that using optical rain gauges to calibrate radars will be particularly difficult as N_0 changes within the rain.

Under extremely heavy rainfall conditions, the optical rain gauge is relatively high when compared to the other rain gauges (Fig. 13). This is consistent with the high

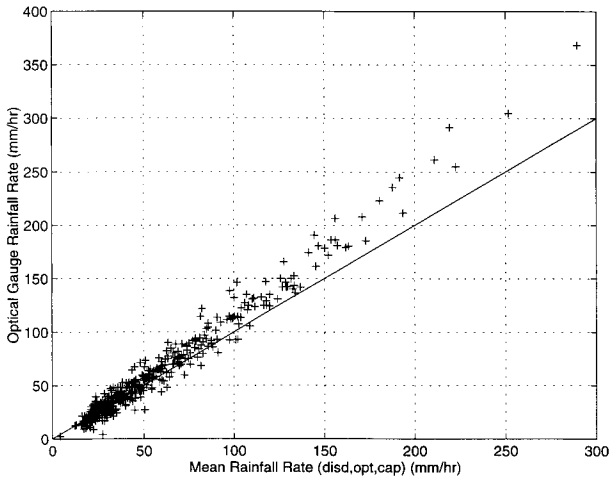

FIG. 13. Optical rain gauge rainfall rates compared to the mean of the optical, disdrometer, and capacitance rain gauges during heavy and extremely heavy rainfall. The data include 444 min of heavy rainfall from Apr, May, Sep, and TS Gordon.

N_0 hypothesis; the rain has relatively more small drops. The other extreme, light rainfall rates, are more difficult to evaluate as the other rain gauges perform marginally at light rainfall rates.

The influence of wind on the optical gauge is also difficult to quantify definitively. The data from TS Gordon show a tendency for the optical gauge to overestimate rainfall rate as wind speed increases, but this result is relative to the other rain gauges, in particular, when compared to the capacitance and disdrometer gauges. But both of these gauges apparently underestimate the rainfall rate as wind speed increases, and thus comparison to them would produce a potentially false result that the optical rain gauge is also sensitive to wind speed. Nothing about the physics of the optical rain gauge suggest that there should be a wind speed dependence. In fact, this feature makes the optical rain gauge an attractive choice for deployment on ships and buoys.

g. The acoustic rain gauge

The acoustic rain sensor is, in fact, an algorithm used to invert the underwater sound field into components associated with four raindrop sizes (small, medium, large, and very large) (Nystuen 1996). Table 2 shows that the acoustic sensor is highly correlated, mean correlation coefficient of 0.90, with the other rain gauges. However, the correlation coefficient is lower than the correlation of the other gauges to each other. In other words, the variability of the acoustic rain measurement is higher than that of the other rain gauges. This scatter is due, in part, to the absence or presence of the extraordinarily loud very large raindrops and the subsequent ability or inability to acoustically detect the relatively quiet smaller raindrops.

The detection of very large raindrops is critical to the success of the acoustic algorithm. The algorithm is, in fact, three different inversions depending on whether or not large and very large raindrops are detected acoustically (Nystuen 1996). When very large raindrops are present within the rain, they dominate the underwater sound field. If they are not accurately counted, then the algorithm compensates by overcounting or undercounting the smaller drop size categories. These drop size categories, especially the medium and large drops, often contain a large fraction of the total water volume in the rain. Based on comparison to the disdrometer data, accurate estimates of the large, medium, and small drop populations when very large drops are present are relatively poor. A simplier algorithm attempting to only measure rainfall rate rather than the full drop size distribution; for example, Nystuen et al. (1993) may be appropriate when very large raindrops are detected. Using the disdrometer data to verify detection of very large raindrops, the acoustic algorithm does correctly detect the absence or presence of very large raindrops 98% of the time.

An example of this problem is shown in Fig. 3 during mins 200–280 of event 150. During this period a few ''undetected'' very large raindrops are present in the rain. The algorithm compensated by overestimating the medium drop category, resulting in overestimations of rainfall rate. A more extreme example of this problem occurred during a 30-min event in February 1994. The overestimation of rainfall rate during this single event resulted in the extremely high regression slope bias (1.65 in Table 3) for that entire month. If the data from that event were removed from the February 1994 dataset, then the regression slope for February 1994 drops from 1.65 to 1.03. Of course, the event is part of the overall dataset.

During extremely heavy rainfall, two additional potential problems affect the acoustic inversion of the underwater sound field. During extremely heavy rainfall, there is acoustic evidence of bubbles being trapped underwater. For example, during event 150 (Fig. 3, Mins 60–70), the sound field above 40 kHz becomes ''quieter'' during the intense downpour. This is explained by the formation a layer of bubbles between the surface and the hydrophone. Such a layer of bubbles would absorb the sound of subsequent raindrops arriving at the surface, distorting the measured sound field and making its acoustic inversion more difficult.

The other potential problem occurring during extremely heavy rainfall is extreme surface roughness on the length scale of a raindrop splash. The acoustic inversion assumes that the drops are striking a flat water surface. This is a good assumption under almost all rainfall situations. However, under extremely heavy rainfall rates, the drop flux N_f reaches 10^4 m^{-2} s^{-1} (Fig. 2). This suggests extreme surface roughness on the length scale of a raindrop splash. This roughness is likely to affect the physics of individual drop splashes and

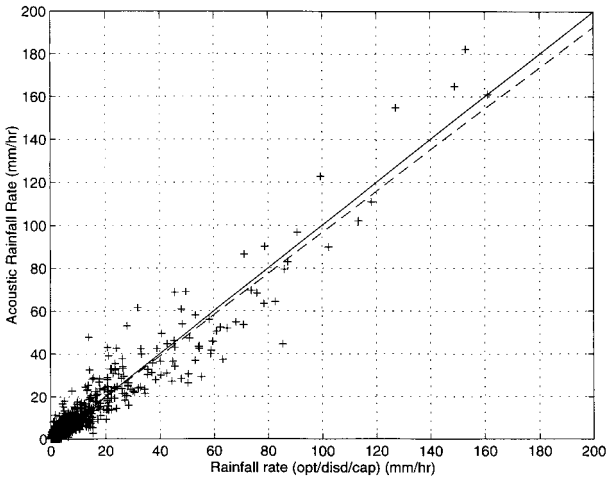

FIG. 14. Modified acoustical rainfall rates compared to the mean of the disdrometer, optical and capacitance rain gauges during TS Gordon. The acoustic algorithm was modified to adjust for the quieter mean conditions that prevailed during TS Gordon. The bias (slope of the first-order regression) of the acoustical rainfall rate measurements is 0.96 and the correlation coefficient is 0.94. Very few situations of large median drop diameter, D_0, occurred in TS Gordon, allowing the acoustic inversion to perform well.

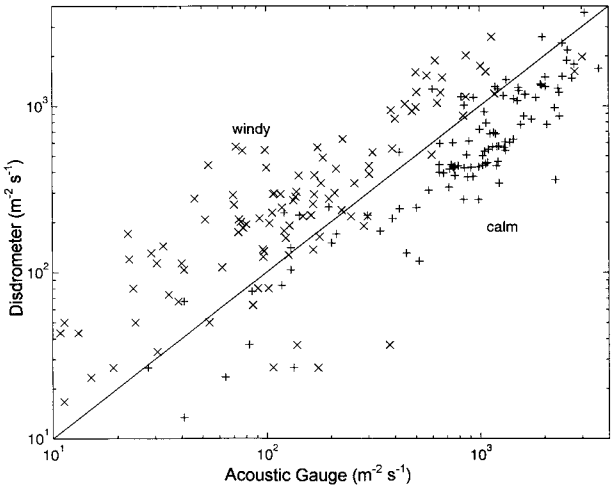

FIG. 15. The influence of wind on the small drop population estimates by the acoustic inversion and the disdrometer. The acoustic small populations estimates during calm conditions, $U < 2$ m s^{-1}, ''+'' symbols, are higher by a factor of 3 than during windy conditions, $U > 5$ m s^{-1}, the ''×'' symbols.

may change the basis functions for the acoustic inversion for the different drop size categories.

Estimating the medium drop size population category is difficult as long as large drops are present in the rain. Medium-sized drops simply do not make much sound underwater and are therefore hard to measure acoustically. It may be better to estimate their population by interpolation of the louder large and small drop categories. Research into this issue is ongoing. Note, that the small drop populations are measured fairly accurately because these drops are actually louder and have a distinctive sound signature when compared to the medium drops.

Another drop size category, which cannot be measured acoustically, is the tiny drop category (<0.8 mm diameter). These drops do not make detectable sound underwater (see Fig. 1) and therefore can not be acoustically measured. Fortunately, the amount of rain volume in this drop size category is almost always small and so the inability of the acoustic method to measure this size category only introduces a small error. Only one example of a rain consisting of mostly tiny raindrops exists in the entire dataset (Fig. 1). Most drizzle situations contain some small drops and are easily detected and measured acoustically.

The bias shown in Table 3 for the TS Gordon dataset is 0.55. The mean wind conditions were higher in this dataset than in any other data considered. The underestimation of rainfall rate was consistent throughout the dataset and was due to an underestimation of the small, medium, and large drop populations. In effect, the sound levels produced by all drop sizes were quieter than expected. By ''tuning'' the acoustic algorithm to these quieter conditions, the performance of the acoustic algorithm improved markedly (Fig. 14). The bias is 0.96 and the correlation to the other gauges is 0.94. The variance of the acoustic rainfall rate measurements is lower when compared to the other datasets. TS Gordon had the lowest occurrence of high median drop diameter, D_0, of any of the datasets. The relative absence of very large raindrops within this dataset may help to explain the lower variance of this dataset when compared to the other datasets. By adjusting the acoustic inversion algorithm, the influence of wind on it can be further examined.

The sound production mechanism of the small drops is known to be sensitive to angle of impact of the raindrop (Medwin et al. 1990; Nystuen 1993). For this reason wind is expected to affect the measurement of small raindrop populations. Figure 15 shows the influence of wind on the small drop population estimates during TS Gordon. The acoustic measurement of small drop populations is a function of wind speed. As the wind speed increases from ''calm'' conditions ($U < 2$ m s^{-1}) to ''windy'' conditions ($U > 5$ m s^{-1}), the small drop population estimates when compared to the disdrometers estimates decreased by a factor of three. The medium and large drop populations estimates do not show this wind speed dependence, although the tuning of the algorithm to the TS Gordon dataset may reflect a ''wind speed'' dependence for sound generation by all raindrop sizes.

5. Conclusions and recommendations

a. Summary

Rainfall rate data from six different types of automatic rain gauges collected over a 17-month period from Sep-

tember 1993 to January 1995 in Miami, Florida, have been examined to identify rainfall conditions that affect the performance characteristics of each type of gauge. These data were subdivided into nine datasets (8 months and a 3-day period when TS Gordon visited Miami) covering 9102 minutes. Rain gauge types include disdrometer, optical, capacitance, weighing, tipping bucket, and underwater acoustic inversion. For each instrument, the data were converted to 1-min rainfall rates to facilitate intercomparison.

A wide variety of rainfall conditions were recorded. These included wintertime stratiform frontal rainfall, intense springtime convective systems with extremely high rainfall rates (over 100 mm h^{-1}), summertime convective storms, mesoscale convective systems in the rainy season (September–October), and one tropical storm (TS Gordon). The disdrometer data were used to calculate several descriptive rainfall parameters including N_0, the *y* intercept of the Marshall–Palmer drop size distribution function [Eq. (2)], and D_0, the median drop size by volume [Eq. (10)]. The data were also subdivided by wind speed and rainfall rate, although the range of wind speeds recorded at the experiment site was limited.

All of the rain gauges performed well, with intercorrelations of order 0.9 or higher and biases of less than 10%. However, each system showed limitations:

The disdrometer does not ''count'' tiny raindrops in high ambient noise situations, including extremely heavy rainfall and high wind situations. These were also times when the disdrometer underestimated rainfall rate relative to the other gauges. Extrapolating to include the ''uncounted'' tiny raindrops does not correct this underestimation of rainfall rate.

The capacitance gauge performed well throughout the experiment, although its 1-min rainfall rate measurement did exhibit increased ''noise'' during light rain or high wind conditions.

Another collection-type gauge in the system is a tipping bucket rain gauge. This is the only type of automatic rain gauge in widespread operational use. It cannot resolve light or moderate rainfall rates ($R < 5$ mm h^{-1}) at a one-minute time interval. Under extremely high rainfall rates, it underestimated rainfall rate relative to the other rain gauges.

The optical rain gauge measures rainfall rate, rather than an accumulation. It is sensitive to the relative distribution of small to large raindrops within the rain. Although not strictly mathematically correct, the rainfall parameter N_0 [Eq. (2)] appears to physically describe this feature of the drop size distribution. When N_0 was high (over 20 000), indicating relatively more small drops in the rain, the optical rain gauge overestimated rainfall rate relative to the other gauges. This occurred during one light drizzle and during extremely heavy (over 100 mm h^{-1}) rainfall. When N_0 was small (under 5000), the optical rain gauge underestimated rainfall rate relative to the other gauges, often at the start of convective events when the rain consisted of relatively few, but large to very large raindrops ($D_0 > 2$ mm) and during stratiform rain associated with mesoscale convective systems. The optical rain gauge biased high *relative to* the other rain gauges during higher winds, but the other gauges are suspected of underestimating rainfall rate during windy conditions.

The acoustic rainfall measurement depends on underwater sound production by individual raindrop splashes. It showed more variability than the other rain gauges (lower correlation coefficients when intercompared to the other gauges) and biases that could persist over individual rain events, causing a wide range of apparent bias from dataset to dataset (see Table 3). An important factor affecting the acoustic measurement is the presence or absence of very large raindrops (over 3.5-mm diameter) within the rain. These raindrops are extraordinarily loud underwater and, when they are present, make accurate counts of the smaller drop populations difficult. Accurate measurement of the medium drop size category (1.2–2.0-mm diameter) is particularly difficult as these drops do not produce much sound underwater; however the small drop size category (0.8–1.2-mm diameter) is loud and easily detected underwater. The physics of the sound production mechanism for small drops is affected by wind.

b. Recommendations for deployment of rain gauges on ocean buoys

The need for surface measurements of precipitation in oceanic regions is well recognized. To date, the best in situ rainfall measurements are qualitative present weather ship observation; see, for example, Petty (1995). Rain gauges deployed on ships and buoys have not performed well. This is mostly because of wind exposure, platform stability problems, and the lack of availability of appropriate automatic rain gauges. Now that several types of automatic rain gauges exist, it is possible to comment on their likely performance characteristics on buoys.

Two of the collection-type gauges, the weighing and tipping bucket gauges, directly depend on gravity to make the rainfall measurement. Unfortunately, platform accelerations due to ocean surface waves, make such measurements difficult or impossible on buoys. The tipping bucket gauge is particularly unsuited to this environment and should not be considered for buoy deployment. The capacitance gauge does not depend directly on gravity; however, water motion within the chamber will lead to instrument noise. This was observed under windy conditions during this experiment, presumably due to the vibration of the instrument by the wind. This suggests that measurements of light rainfall rates by this sensor will require longer temporal averaging to reduce this instrument noise. Furthermore, all of the collection-type gauges will experience un-

derestimation due to the wind-exposure/catchment problems known to affect this type of gauge.

The physics of the measurement of rainfall by an optical rain gauge suggest that it should not be as affected by wind as the other gauges. However, evaluation of this possibility could not be rigorously examined with these data. These gauges were deployed during the Tropical Ocean and Global Atmosphere Coupled Ocean–Atmosphere Response Experiment (TOGA-COARE) (McPhaden and Milburn 1992) but gave erratic results that remain unresolved and an ongoing research topic. The influence of changes in the drop size distribution on the rainfall rate measurement of this gauge apply to any deployment situation and represent an inherent variability using this type of instrument.

The disdrometer also has potential for deployment at sea. The type used in this experiment (Joss–Waldvogel type) is not seaworthy; however, a new design is available (Rowland 1976). The mechanical nature of the measurement, a conversion of vertical drop momentum into drop size, suggest that platform motion might affect the measurement of drop size. The data considered here show an underestimation during higher wind situations and may be an indication that the disdrometer will perform poorly in a high wind exposure situation on a buoy.

Finally, the acoustic measurement of rain is inherently available from an oceanic mooring or autonomous drifter. Ship noise may make this measurement unavailable from ships. This measurement type has a higher variability than the other rain gauges considered here, but would be unaffected by platform stability problems. It is affected by wind, especially the measurement of small drops, although acoustic detection of rainfall at sea is documented even under high wind conditions (Nystuen and Farmer 1989; Nystuen and Selsor 1997). Under calm wind conditions, light rain is easily detected.

In summary, four of the automatic rain gauges considered here have potential for deployment on buoys: the optical, capacitance, disdrometer, and acoustic rain gauges. Of these, platform stability problems will affect instrument noise for the capacitance gauge and the disdrometer. Wind exposure is likely to affect the capacitance gauge, the disdrometer, and the acoustic system. Variations in drop size distributions within the rain will affect the optical and acoustic systems. It should be emphasized that the rain gauges evaluated here were deployed on land. They need to be intercompared on buoys.

Acknowledgments. The rainfall experiment was established through the efforts of John Proni (NOAA/AOML), Peter Black (NOAA/AOML) and John Wilkerson (NOAA/NESDIS). Engineering support was provided by Jeff Bufkin, Charles Lauter, Ulises Rivero, Jack Stamates, and Mark Boland, AOML. Timothy Hiett, Hanscom AFB, loaned the disdrometer to AOML. Funding for data analysis was provided by the National Data Buoy Center, NOAA, and the National Science Foundation, Ocean Instrumentation Division.

REFERENCES

Arkin, P. A., and P. Xie, 1994. The global precipitation climatology project: First algorithm intercomparison project. *Bull. Amer. Meteor. Soc.,* **75,** 401–419.

Atlas, D., and C. W. Ulbrich, 1974: The physical basis for attenuation rainfall relationships and the measurement of rainfall parameters by combined attenuation and radar methods. *J. Rech. Atmos.,* **8,** 275–298.

Barrett, E. C., J. Dodge, M. Goodman, J. Janowiak, and E. Smith, 1994: The First WetNet Intercomparison Project (PIP-1). *Remote Sens. Rev.,* **11,** 49–60.

——, C. Kidd, and D. Kniveton, 1995: The First Wetnet Precipitation Project (PIP-1): Reflections on the results. *Proc. IGARSS'95,* Vol 1, Firenze, Italy, IGARSS, 649–651.

Dorman, C. E., and R. H. Bourke, 1979: Precipitation over the Pacific Ocean, 30°S to 60°N. *Mon. Wea. Rev.,* **107,** 896–910.

Ebert, E. E., M. J. Manton, P. A. Arkin, R. J. Allam, G. E. Holpin, and A. Gruber, 1996: Results from the GPCP Algorithm Intercomparison Programme. *Bull. Amer. Meteor. Soc.,* **77,** 2875–2887.

Holmes, J., and E. Michelena, 1983: Design and testing of a new rain gauge for NDBC meteorological data buoys. Preprints, *Fifth Symp. on Meteorological Observations and Instrumentation,* Toronto, ON, Canada, Amer. Meteor. Soc., 34–37.

——, B. Case, and E. Michelena, 1981: Rain Gauge for NOAA data buoys. *IEEE/MTS Symp. Oceans '81,* Boston, MA, Mar. Tech. Soc., 463–467.

Houze, R. A., Jr., 1989: Observed structure of mesoscale convective systems and implications for large scale heating. *Quart. J. Roy. Meteor. Soc.,* **115,** 425–461.

Joss, J., and A. Waldvogel, 1967: Ein Spektrograph für Niederschlagstropfen mit automaticscher Auswertung. *Pure Appl. Geophys.,* **68,** 240–246.

——, and ——, 1969: Raindrop size distribution and sampling size errors. *J. Atmos. Sci.,* **26,** 566–569.

Legates, D. R., and C. J. Willmott, 1990: Mean seasonal and spatial variability in gauge corrected global precipitation. *Int. J. Climatol.,* **10,** 111–127.

——, and T. L. deLiberty, 1993: Precipitation measurement biases in the United States. *Water Resour. Bull.,* **29,** 855–861.

Marshall, J. S., and W. M. Palmer, 1948: The distribution of raindrops with size. *J. Meteor.,* **5,** 165–166.

Marselek, J., 1981: Calibration of the tipping-bucket raingage. *J. Hydrol.,* **53,** 343–354.

McPhaden, M. J., and H. B. Milburn, 1992: Moored precipitation measurements for TOGA. *TOGA Notes* **7,** 1–5.

Medwin, H., A. Kurgan, and J. A. Nystuen, 1990: Impact and bubble sound from raindrops at normal and oblique incidences. *J. Acoust. Soc. Amer.,* **88,** 413–418.

——, J. A. Nystuen, P. W. Jacobus, D. E. Snyder, and L. H. Ostwald, 1992: The anatomy of underwater rain noise. *J. Acoust. Soc. Amer.,* **92,** 1613–1623.

Milburn, H. B., P. D. McLain, and C. Meinig, 1996: ATLAS buoy—Reengineered for the next decade. *Proc. IEEE Oceans'96,* Fort Lauderdale, FL, IEEE, 698–702.

Nystuen, J. A., 1993: An explanation of the sound generated by light rain in the presence of wind. *Natural Physical Sources of Underwater Sound,* B.R. Kerman, Ed., Kluwer Academic Publishers, 659–668.

——, 1996: Acoustical rainfall analysis: Rainfall drop size distribution using the underwater sound field. *J. Atmos. Oceanic Technol.,* **13,** 74–84.

——, and D. M. Farmer, 1989: Precipitation in the Canadian Atlantic Storms Program: Measurements of the acoustic signature. *Atmos.–Ocean,* **27,** 237–257.

——, and H. Medwin, 1995: Underwater sound generated by rainfall: Secondary splashes of aerosols. *J. Acoust. Soc. Amer.*, **97,** 1606–1613.
——, and H. D. Selsor, 1997: Weather classification using passive acoustic drifters. *J. Atmos. Oceanic Technol.*, **14,** 656–666.
——, C. C. McGlothin, and M. S. Cook, 1993: The underwater sound generated by heavy precipitation. *J. Acoust. Soc. Amer.*, **93,** 3169–3177.
——, J. R. Proni, C. A. Lauter, J. Bufkin, U. Rivero, M. Boland, and J. C. Wilkerson, 1994: APL Disdrometer Evaluation. NOAA Tech. Memo. ERL AOML-83, 43 pp.
——, ——, P. G. Black, and J. C. Wilkerson, 1996: A Comparison of Automatic Rain Gauges. *J. Atmos. Oceanic Technol.*, **13,** 62–73.
Petty, G. W., 1995: Frequencies and characteristics of global oceanic precipitation from shipboard present-weather reports. *Bull. Amer. Meteor. Soc.*, **76,** 1593–1616.
Pruppacher, H. R., and J. D. Klett, 1978: *Microphysics of Clouds and Precipitation.* Reidel, 714 pp.
Reed, R. K., and W. P. Elliot, 1979: New precipitation maps for the North Atlantic and North Pacific Oceans. *J. Geophys. Res.*, **84,** 7839–7846.
Rowland, J. R., 1976: Comparison of two different raindrop disdrometers. *17th Conf. on Radar Meteorology*, Seattle, WA, Amer. Meteor. Soc., 398–405.
Sheppard, B. E., and P. I. Joe, 1994: Comparison of raindrop size distribution by a Joss–Waldvogel disdrometer, a PMS 2DG spectrometer and a POSS Doppler radar. *J. Atmos. Oceanic Technol.*, **11,** 874–887.
Tokay, A., and D. A. Short, 1996: Evidence from tropical raindrop spectra of the origin of rain from stratiform versus convective clouds. *J. Appl. Meteor.*, **35,** 355–371.
Tucker, G. B., 1961: Precipitation over the North Atlantic Ocean. *Quart. J. Roy. Meteor. Soc.*, **87,** 147–158.
Ulbrich, C. W., 1983: Natural variations in the analytical form of the raindrop size distribution. *J. Climate Appl. Meteor.*, **22,** 1764–1775.
——, 1985: The effects of drop size distribution truncation on rainfall integral parameters and empirical relations. *J. Climate Appl. Meteor.*, **24,** 580–590.
——, and D. Atlas, 1978: The rain parameter diagram: Methods and applications. *J. Geophys. Res.*, **83,** 1319–1325.
Waldvogel, A., 1974: The N_0 jump of raindrop spectra. *J. Atmos. Sci.*, **31,** 1068–1078.
Wang, T. I., and S. F. Clifford, 1975: Use of rainfall-induced optical scintillations to measure path-averaged rain parameters. *J. Opt. Soc. Amer.*, **65,** 927–937.
——, G. Lerfald, R. S. Lawrence, and S. F. Clifford, 1977: Measurement of rain parameters by optical scintillation. *Appl. Opt.*, **16,** 2236–2241.
——, K. B. Earnshaw, and R. S. Lawrence, 1978: Simplified optical path-averaged rain gauge. *Appl. Opt.*, **17,** 384–390.
Willis, P. T., 1984: Functional fits to some observed drop size distributions and parameterization of rain. *J. Atmos. Sci.*, **41,** 1648–1661.